CHEMISTRY
A EUROPEAN JOURNAL

DOI: 10.1002/chem.200600075

Reactions of Th and U Atoms with C_2H_2: Infrared Spectra and Relativistic Calculations of the Metallacyclopropene, Actinide Insertion, and Ethynyl Products

Lester Andrews,*[a] Gary P. Kushto,[a, b] and Colin J. Marsden[c]

Abstract: Reactions of laser-ablated Th and U atoms with C_2H_2 during condensation with excess argon at 7 K give several new product species. The metallacyclopropene, inserted hydride, and actinide ethynyl are identified from isotopic frequencies and relativistic DFT calculations. The higher-energy vinylidine isomer was not observed. These actinide metallacyclopropenes exhibit substantially stronger bonding interactions than found recently for the Pd and Pt metals. In the case of Th(C_2H_2) the argon matrix interaction is strong enough to reverse the computed order of states (MR-CISD) in favor of a triplet ground state for the $(Ar)_n$(Th-(C_2H_2)) complex. The nature of the electronic interactions between various metal atoms and acetylene is compared and the origin of the particularly strong interaction for U and Th is traced to the higher energy of their 6d orbitals. The ThCCH and UCCH actinide ethynyl products are also observed and characterized by C≡C stretching modes 38 ± 2 cm^{-1} lower than acetylene itself.

Keywords: density functional calculations · IR spectroscopy · matrix isolation · thorium · uranium

Introduction

Adsorption and reactions of C_2H_2 on metal surfaces have been studied thoroughly owing to the industrial importance of hydrocarbon hydrogenation and dehydrogenation processes.[1–3] Although the catalytic transition metals have received the most attention in this regard, actinide metals are very reactive, based on our experience with U and Th atom reactions with such small molecules as O_2, N_2, H_2, CO and methane.[4–14] How will Th and U interact with C_2H_2, where metallacyclopropene, metalvinylidine and HMCCH insertion products are all possible? Metallacyclopropenes have been observed for Li, In, Ti, Ni, Pd and Pt where these molecules have been identified by vibrational spectroscopy and characterized by C=C stretching modes at 1655, 1668, 1364, 1647, 1710 and 1654 cm^{-1}, respectively, which are all substantially lower than the C≡C stretching mode for C_2H_2 at 1974 cm^{-1}.[15–22] Furthermore, the possibility of additional d and f to π* interaction for Th and U with C_2H_2 and forming actinide cyclopropenes stimulates our interest in these reaction products.[23] In addition, will the vinylidine isomer be more stable for the actinide as it is for the third row metal Pt?

While the use of matrix-infrared spectroscopy for the identification of new reactive molecular species spans from the present back five decades,[24] the performance and reliability of computational methods has been put to the test more recently particularly in the actinide field. A variety of theoretical methods ranging from the straightforward DFT to the more sophisticated MOLCAS and CASPT2 have been employed to investigate known large actinide complexes as well as new small molecules, and we list some recent examples.[25–37] The simple DFT approach appears to work well in many cases, particularly for the prediction of vibrational frequencies, and in the case of UO_2, uranium dioxide, DFT in combination with matrix IR spectroscopy, first identified the $^3\Phi$ ground state.[4,26] It is therefore important to compare vibrational frequencies calculated by simple methods such as density functional theory with observed fre-

[a] Prof. Dr. L. Andrews, Dr. G. P. Kushto
Department of Chemistry
P.O. Box 400319, University of Virginia
Charlottesville, VA 22904-4319 (USA)
Fax: (+1) 434-924-3710
E-mail: lsa@virginia.edu

[b] Dr. G. P. Kushto
Present address: Naval Research Laboratory
Washington, DC 20375 (USA)

[c] Prof. Dr. C. J. Marsden
Laboratoire de Physique Quantique, UMR 5626, IRSAMC
Université Paul Sabatier, 118 Route de Narbonne
31062 Toulouse Cedex 4 (France)

Supporting information for this article is available on the WWW under http://www.chemeurj.org/ or from the author: Table S1.

quencies for new species, including those involving heavy metals, which present a particular challenge, due to the importance of relativistic effects. Such calculations have successfully modeled vibrational frequencies for a number of small thorium and uranium-containing molecules.[4–14]

Experimental and Computational Methods

The laser-ablation and matrix-isolation experiment has been described previously.[4,9,38] The Nd/YAG laser fundamental (1064 nm, 10 Hz repetition rate, 10 ns pulse width) was focused on rotating actinide metal target (Oak Ridge National Laboratory) using 5–20 mJ per pulse. Laser-ablated actinide atoms were co-deposited with C_2H_2 (typically 0.25%) in excess argon onto a 7 K CsI window at 2–3 mmol for one hour. Acetylene (Matheson, distilled to remove acetone stabilizer), C_2D_2 (Cambridge Isotopic Laboratories) and $^{13}C_2H_2$ (MSD Isotopes) were used in different experiments. Infrared spectra were recorded at 0.5 cm^{-1} resolution on a Nicolet 550 spectrometer with 0.1 cm^{-1} accuracy using a HgCdTe detector. Matrix samples were irradiated with a medium-pressure mercury arc lamp (Philips, 175W, globe removed, $\lambda >$ 220 nm) and annealed at different temperatures to allow diffusion and further association of metal atoms and acetylene.

Density functional theory calculations were done for expected product molecules using the Gaussian 03 program system.[39] Standard all-electron triple-zeta basis sets were used for C and H,[40] augmented with polarization functions (d-type exponent 0.75 for C, p-type exponent 0.9 for H), while "very small-core" pseudopotentials were adopted for Th and U (60 electrons treated as "core", corresponding to those in atomic orbitals whose principal quantum number is less than 5), together with the associated flexible basis sets.[41] Three different versions of density functional theory were employed: B3LYP,[42] PW91 and B3PW91.[43] The "ultrafine" grid was used for all the calculations of vibrational frequencies that are reported here. A few calculations of the coupled-cluster type (CCSD and CCSD(T)) were undertaken,[44] sometimes with geometry optimization, for purposes of comparison. In these calculations, excitations out of the 11 lowest-energy occupied orbitals and into their virtual counterparts were excluded. Multi-reference calculations at the CASSCF and MR-CISD levels were performed for Th-(C_2H_2) with the MOLPRO program[45] using the B3LYP structures to obtain a more reliable singlet-triplet state energy difference.

Results

Infrared spectra of laser-ablated Th and U reaction products with C_2H_2, and DFT structure and vibrational frequency calculations of product molecules will be presented.

Th+C_2H_2: Infrared spectra of thorium and acetylene reaction products in solid argon are illustrated in Figure 1; the product absorptions are listed in Table 1. Weak ThO and ThO_2 absorptions at 876.3 and 787.1 cm^{-1} (not shown), and weak ThH and ThH_2 absorptions at 1485.1 and 1455.9 cm^{-1} and $Th(N_2)_2$ at 1895.5 cm^{-1} were observed.[5,7] Infrared absorptions for C_4H_2, the CCH radical, cation and anion are common to laser-ablated metal and acetylene experiments.[46–49] A weak HCO band[50] appears at 1862 cm^{-1} on annealing and it attests the formation of H atoms for the fa-

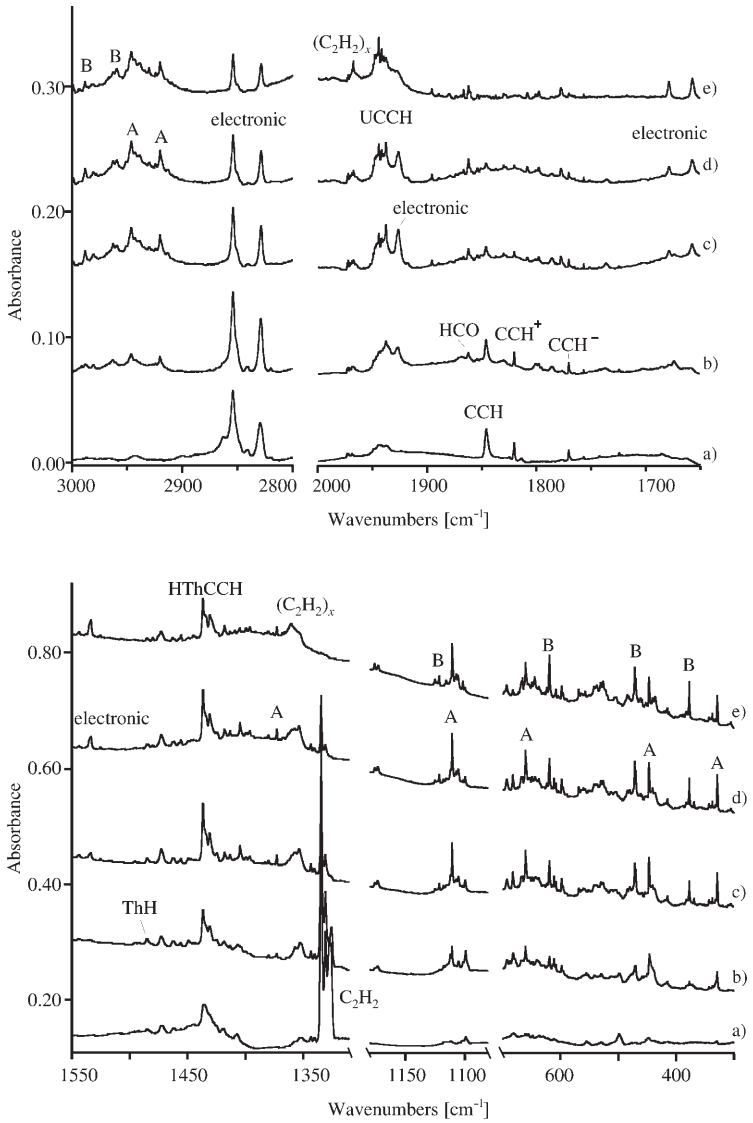

Figure 1. Infrared spectra in the 3000–2800, 2000–1650, 1550–1310, 1180–1080, and 650–450 cm^{-1} regions for laser-ablated Th co-deposited with 0.25% C_2H_2 in argon at 7 K. a) Sample deposited for 1.5 ; b) after annealing to 23 K; c) after annealing to 28 K; d) after annealing to 34 K; e) after annealing to 43 K.

Table 1. Product absorptions [cm^{-1}] observed from laser-ablated thorium atom reactions with acetylene in excess argon.

Assignment	$^{12}C_2H_2$	$^{13}C_2H_2$	$^{12}C_2D_2$
C_4H_2	3325.4	3308.8	2593
$Th(C_2H_2)_2$	2988.2	2975.1	
$Th(C_2H_2)_2$	2962.2	2954.1	
$Th(C_2H_2)$	2946.2	2935.2	2168.5
$Th(C_2H_2)$	2920.2	2912.3	2151.8
electronic	2854	2854	2854
electronic	2829	2829	2829
H_2CCO	2142	2080	2112
C_4H	2060.4	1981.5	2049.4
C_3 (weak)	2039	1963.8	2039
HCCO (weak)	2019.2	1961.4	1989.8
$(C_2H_2)_x$ (weak)	1972, 1967	1908, 1904	1760, 1755
ThCCH $(C_2H_2)_x$	1944.2	1874.1	1833.5
ThCCH	1937.6	1868.2	1825.8
electronic	–	1937	1937
electronic	1927	1927	1927
CCH	1845.8	1785.5	1746.5
CCH^+	1820.4	1755.1	1724.6
CCH^-	1770.5	1711.8	1676.7
electronic	1679	1679	1679
electronic	1657	1657	1657
electronic	1544	1544	1544
electronic	1534	1534	1534
ThH	1485.1	1485.1	1060.4
HTh-X	1472	1472	1051
ThH_2	1455.9	1455.9	1040
HThCCH	1436.6	1436.6	1027.7
HThCCH (site)	1430.8	1430.8	1022.2
HTh-X	1404.6	1403.8	1002.2
$Th(C_2H_2)$	1373.0	(1322)[a]	1334.2
weak	1173.3	1153.7	948.6
$Th(C_2H_2)_2$	1121.7	1104.7	948.6
$Th(C_2H_2)$	1110.6	1094.5	930
$Th^+(C_2H_2)$	1099.7	1081.3	922.3
$Th(C_2H_2)$	630.2	625.3	473.2
$Th(C_2H_2)_2$	609.7	606.3	
CCH^+	549.5	544.8	433.8
$Th(C_2H_2)_2$	535.9	521.4	468.9
$Th(C_2H_2)$	535.1	520.8	460.9
HTh-X	523.5	506.7	
$Th(C_2H_2)_2$	488.7	473.1	–
$Th(C_2H_2)$	464.5	449.6	–

[a] Masked by $^{13}C_2H_2$: Deduced from calculated isotopic shift.

vorable reaction with trace CO impurity present in all of these experiments. In addition weak absorptions at 1972, 1908, and 1760 cm^{-1} are near the IR-silent fundamental of C_2H_2, $^{13}C_2H_2$, and C_2D_2, and these bands are due to acetylene clusters in the matrix. The above bands increase slightly on annealing and are surpassed on higher temperature annealing by lower bands at 1967, 1904, and 1755 cm^{-1} that are probably due to larger acetylene clusters. No isolated C_2H_2 monomer survives the final 40–43 K annealing cycle. Bands at 2854.0 ± 0.2 and 2829.0 ± 0.3 cm^{-1} increase on 23 K annealing, decrease on $\lambda > 240$ nm irradiation, and decrease on annealing to 33 K and above. These bands show no precursor isotopic shifts, depend on laser energy, and are common to Th experiments with other reactants.[7,14,47] The annealing and photolysis behavior are consistent with a Th_x cluster, and the absorptions are probably due to a d–d electronic transition, as discussed briefly below in the section on Electronic absorptions.

New product absorptions are associated with each other in two major and three minor groups that have different behavior on annealing and photolysis of the deposited solid sample. The major absorption band groups are A (2946.2, 2920.2, 1373.0, 1110.6, 630.2, 535.1 and 464.5 cm^{-1}) and B (2988.2, 2969.5, 1121.4, 609.7, 535.9 and 488.7 cm^{-1}). The A bands are very weak on sample deposition, and the B bands are not observed. The A bands increase markedly and the B bands appear on annealing (Figure 1b), both groups decrease on full arc photolysis (not shown), and both groups increase on further annealing with group B increasing a larger proportion than group A on late annealing (Figure 1c,d). On final annealing group A decreases slightly and group B increases slightly (Figure 1e). The minor group C bands at 1099.7 and 641.3 cm^{-1} are observed on sample deposition, increase on first annealing, and decrease on photolysis and further annealing. Group D absorptions at 1436.6 and 1430.8 cm^{-1} are strong on deposition, sharpen on annealing, increase on photolysis, and decrease slightly on subsequent annealings. The broad E band with sharp 1937.6 cm^{-1} peak increases on annealing and decreases on photolysis, but gives way on final annealings to a sharp 1944.2 cm^{-1} peak. Experiments were done under different conditions of C_2H_2 concentration and laser energy, which affects the Th concentration and plume radiation intensity on the metal surface.

Further investigations were performed with $^{13}C_2H_2$ and C_2D_2. Similar results were obtained, and the isotopic frequencies are compared in Table 1. Figure 2 illustrates spectra for the Th reaction with C_2D_2.

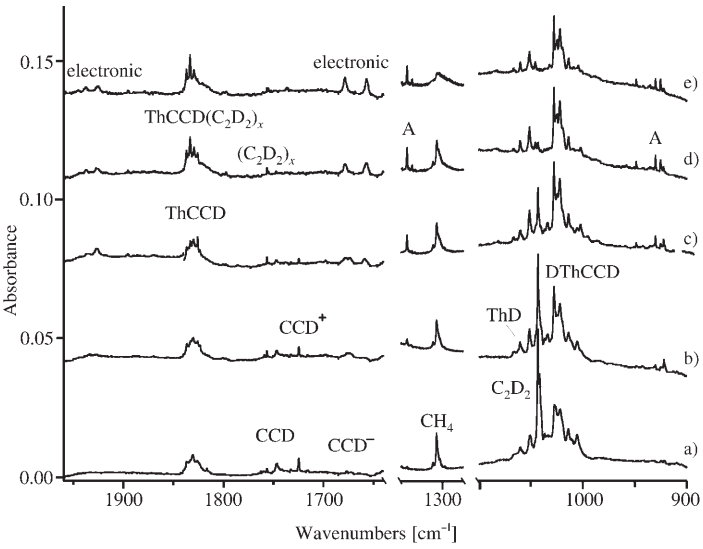

Figure 2. Infrared spectra in the 1960–1640, 1340–1280, and 1100–900 cm^{-1} regions for laser-ablated Th co-deposited with 0.25 % C_2D_2 at 7 K. a) Sample deposited for 1.5 h; b) after annealing to 23 K; c) after annealing to 28 ; d) after annealing to 34 K; e) after annealing to 42 K.

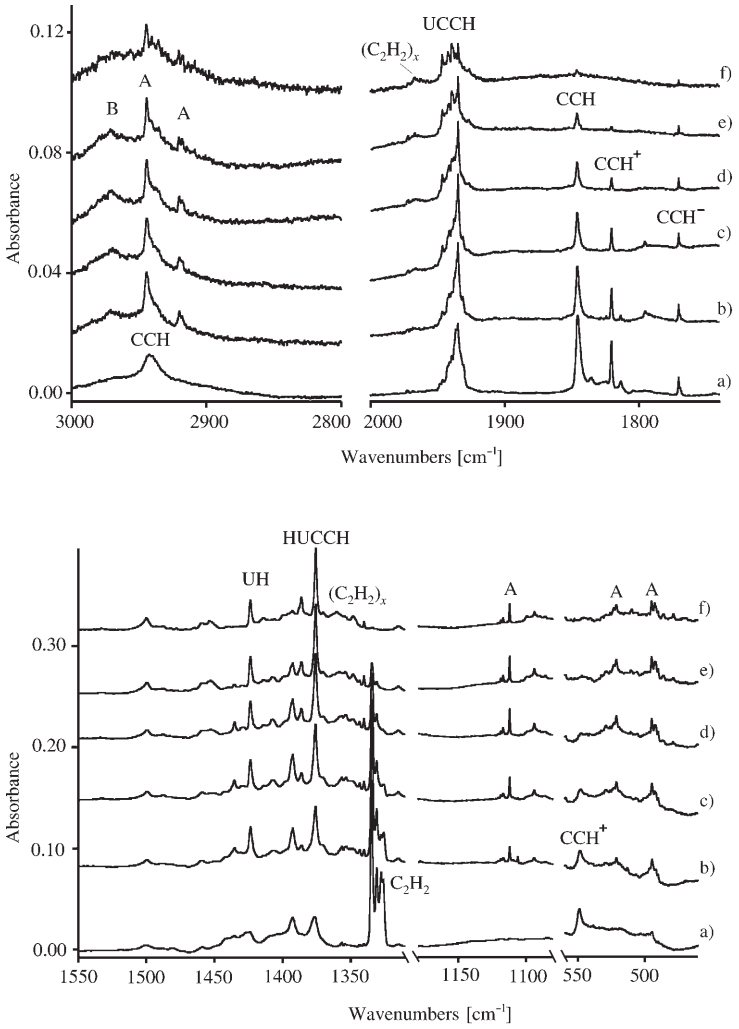

Figure 3. Infrared spectra in the 3000–2800, 2000–1650, 1550–1310, 1180–1080, and 650–450 cm^{-1} regions for laser-blated U co-deposited with 0.25 % C_2H_2 in argon at 7 K. a) Sample deposited for 1.5 h; b) after annealing to 23 K; c) after annealing to 28 K; d) after annealing to 34 K; e) after annealing to 43 K.

U+C_2H_2: Infrared spectra of uranium and acetylene reaction products in solid argon are shown in Figure 3, and the product absorptions are listed in Table 2. The common C_4H_2 and CCH species absorptions were observed,[46,47] and weak UN_2, UO, and UO_2 bands were detected at 1051.0, 819.5 and 776.0 cm^{-1}.[3,4] In addition a weak UH band is observed at 1423.5 cm^{-1}.[6] New product absorptions are arranged by common behavior into one major and four minor groups. Group A (2944.4, 2920.1, 1112.1, 602.9, 521.2, and 494.9 cm^{-1}) bands are extremely weak on sample deposition but grow strongly on annealing, decrease on photolysis, increase on intermediate annealing, and decrease on final annealing just as the analogous Th product. Group B (2970 and 1093.8 cm^{-1}) bands also appear on annealing, decrease on photolysis, and increase more on intermediate annealing than group A before decreasing on final annealing. Group C consists of a single weak 1106 cm^{-1} absorption that increases on early annealing, decreases on photolysis, and decreases markedly on subsequent annealing. Group D bands are observed on sample deposition at 1392.6 and 1375.5 cm^{-1}, the former increases slightly on photolysis, at the expense of the latter and both increase further on intermediate annealing before decreasing on final annealing. Finally, a group E band produced at 1934.9 cm^{-1} on sample deposition increases on first annealing, and decreases on higher annealing with the growth of higher-frequency satellite features.

The spectrum of the U + $^{13}C_2H_2$ reaction is particularly important because a diagnostic group A band falls under the very strong $^{12}C_2H_2$ bending-mode combination band at 1330–1338 cm^{-1}. This group A band appears at 1289.0 cm^{-1} on annealing, below the strong $^{13}C_2H_2$ absorption at 1326 cm^{-1}, along with additional group A bands at 1095.8, 599.1, 507.1, and 477.3 cm^{-1} (Figure 4). Group A bands are also observed in the C–H region at 2932.3 and 2911.9 cm^{-1}. The strong group D bands are not shifted with $^{13}C_2H_2$. Other $^{13}C_2H_2$ counterpart absorptions are listed in Table 2.

The spectrum of U + C_2D_2 reaction products gives group A bands (2164.5, 1303.8, 917.0, 478.5 and 457.5 cm^{-1}), but strongest group D absorptions are shifted to 994.9 and 982.7 cm^{-1} (Figure 5).

Calculations: DFT calculations were first performed for three Th+C_2H_2 isomers, Th–η^2-C_2H_2, $ThCCH_2$ and HThCCH, at the B3LYP level for singlet and triplet states. The global minimum is $^1A_1$ Th(C_2H_2) with $^1A_1$ $ThCCH_2$ 65 kJ mol^{-1} higher and $^1A'$ HThCCH 92 kJ mol^{-1} higher. The $^3A_2$ state (unpaired electrons in a_1 and a_2 orbitals) of Th(C_2H_2) is only 22 kJ mol^{-1} higher, but this state for $ThCCH_2$ is 116 kJ mol^{-1} higher and the $^3A''$ state of HThCCH is 195 kJ mol^{-1} higher. However, with the B3PW91 and PW91 functionals, the $^3A_2$ state of Th(C_2H_2) is only 1 kJ mol^{-1} higher than the $^1A_1$ state.

The B3LYP geometries of the singlet and triplet isomers of Th(C_2H_2) are sketched in Figure 6. Notice that the C–C distances in both species are substantially longer than that calculated for free acetylene (1.201 Å with the same basis and method), but are close to that calculated for free ethyl-

Table 2. Product absorptions [cm^{-1}] observed from laser-ablated uranium atom reactions with acetylene in excess argon.

Assignment	$^{12}C_2H_2$	$^{13}C_2H_2$	$^{12}C_2D_2$
C_4H_2	3325.4	3308.8	2593
$C_2H_2^+$	3104	3095	2311.5
$U(C_2H_2)_2$	2971		
$U(C_2H_2)$	2944.4	2932.9	2164.5
CCH	2942		
$U(C_2H_2)$	2920.1	2911.6	–
H_2CCO	2142	2080	2112
CCH	2105	2053	–
C_4H	2060.4	1981.5	2049.4
C_3 (weak)	2039	1963.8	2039
HCCO (weak)	2019.2	1961.4	1989.8
$(C_2H_2)_x$ (weak)	1972, 1967	1908, 1904	1760, 1755
$UCCH(C_2H_2)_x$	1939	1871	1829
UCCH	1934.9	1867.3	1825.9
CCH	1845.8	1785.5	1746.5
CCH^+	1820.4	1755.1	1724.6
CCH^-	1770.5	1711.8	1676.7
UH (site)	1435.4	1435.4	1025.1
UH	1423.5	1423.5	1016.1
HUCCH (site)	1392.6	1392.6	994.9
HUCCH	1375.5	1375.5	982.7
$U(C_2H_2)$	(1337)[a]	1289.0	1303.8
$U(C_2H_2)$	1112.1	1095.8	917.0
$U^+(C_2H_2)$	1106.1	1089.5	
$U(C_2H_2)_2$	1093.8	1076.9	
HUCCH	674.3		
HUCCH	664.2	658.1	526.6
C_4H_2	627.5	622.4	495.6
$U(C_2H_2)$	602.9	599.1	
CCH^+	549.5	544.8	433.8
$U(C_2H_2)$	521.2	507.1	457.5
$U(C_2H_2)$	494.9	477.3	478.5

[a] Masked by C_2H_2: Deduced from calculated isotopic shift and detected after annealing to 43 K to allow C_2H_2 to diffuse and aggregate.

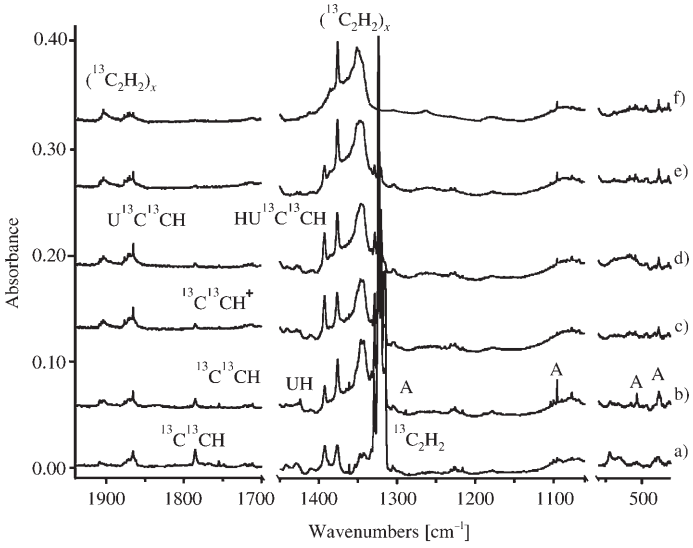

Figure 4. Infrared spectra in the 3000–2800, 2000–1650, 1550–1310, 1180–1080, and 650–450 cm^{-1} regions for laser-ablated U co-deposited with 0.25 % $^{13}C_2H_2$ in argon at 7 K. a) Sample deposited for 1.5 h; b) after annealing to 25 K,; c) after $\lambda > 240$ nm irradiation for 30 min; d) after annealing to 30 K; e) after annealing to 35 K; f) after annealing to 40 K.

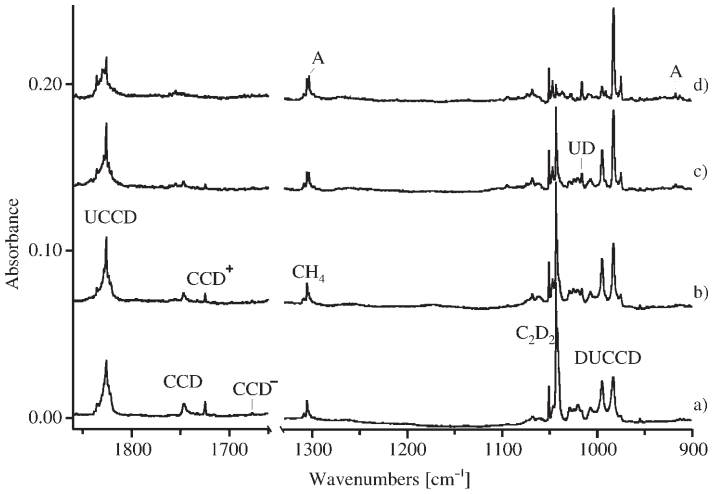

Figure 5. Infrared spectra in the 1860–1660 and 1330–900 cm^{-1} regions for laser-ablated U co-deposited with 0.25 % C_2D_2 in argon at 7 K. a) Sample deposited for 1.5 h; b) after annealing to 25 K; c) after annealing to 33 K; d) after annealing to 39 K.

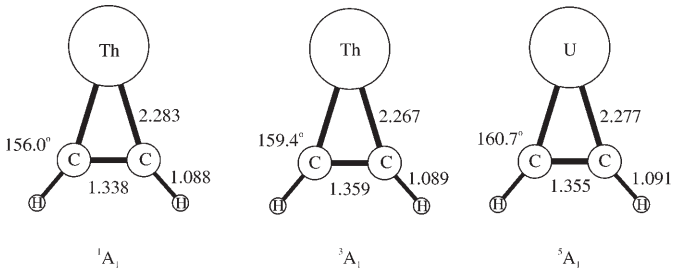

Figure 6. Structures calculated for $Th(C_2H_2)$ and $U(C_2H_2)$ states at the B3LYP level of theory.

ene (1.328 Å). The most significant orbitals for the singlet are the HOMO−1 and HOMO, which have b_2 and a_1 symmetries, respectively, while the LUMO has a_2 symmetry. The HOMO−1 involves an interaction between an in-plane d orbital on Th ($6d_{yz}$ if the atoms are in the y,z plane) and the y component of the π^* C–C antibonding orbital of acetylene. This orbital therefore corresponds to the "back-donation" interaction between Th and acetylene, which significantly weakens the triple bond. The HOMO is essentially a lone pair on Th, of hybrid 7s/6d character, oriented away from the acetylene. Since the back-donation interaction is much stronger than that involving donation from acetylene to Th, the metal atom acquires an appreciable net positive charge (0.39 or 1.35 electrons, according to the Mulliken[51] or NBO[52] analyses, respectively: as there are quite diffuse functions in the basis set, and since the numerical values Mulliken-type populations are very sensitive to the presence of such functions, we think that the "natural" or NBO populations are more realistic). Finally, the calculated dipole moment is 1.66 D.

The $^3A_2$ state of $Th(C_2H_2)$ is obtained from the singlet by the HOMO–LUMO single excitation. As the a_2 orbital that is now singly occupied is essentially a d-type atomic orbital,

strongly localized on Th, the geometries of the two states are very similar, as are the charge distributions (the net charge on Th in the triplet state is +0.48 or +1.48 e, at the Mulliken or NBO levels, respectively). The dipole moment is accordingly larger at 3.18 D. The spin density on Th is 1.95 electrons, another indication of the localized nature of the unpaired electrons.

Vibrational frequencies were computed for the $^1A_1$ and $^3A_2$ states of $Th(C_2H_2)$ using the B3LYP, B3PW91 and PW91 functionals. In most cases, the differences found between B3LYP and B3PW91 frequencies were small (5–15 cm^{-1}), so only the B3LYP and PW91 values are reported in Table 3. Frequencies calculated for the $Th(^{13}C_2H_2)$ and $Th(C_2D_2)$ isotopic products are also compared for the B3LYP functional in Table 3. In addition, vibrational frequencies are given in Table 4 for the higher-energy $ThCCH_2$ and HThCCH isomers. These results are compared with the experimental data in the Discussion section.

Table 3. Frequencies [cm^{-1}] computed for the low lying $^1A_1$ and $^3A_2$ states of $Th(C_2H_2)$ using DFT.

$^1A_1$			$^3A_2$			
PW91	B3LYP	OBS	PW91	B3LYP	B3LYP	B3LYP
3068	3133 (a_1, 24)[a]	2946[b]	3070	3122.6 (a_1, 21)[a]	3111.9[c]	2324.1[d]
3041	3106 (b_2, 13)	2920	3045	3096.8 (b_2, 12)	3088.3	2276.7
1440	1478 (a_1, 2)	1373	1302	1380.5 (a_1, 25)	1330.5	1340.6
1080	1124 (b_2, 39)	1111	1074	1125.6 (b_2, 27)	1108.6	946.5
957	995 (a_2, 0)	–	906	966.5 (a_2, 0)	958.7	765.3
801	843 (a_1, 0.1)	–	784	832.7 (a_1, 0)	831.9	602.3
637	658 (b_1, 45)	630	617	642.6 (b_1, 73)	638.8	485.4
524	524 (a_1, 40)	535	525	521.7 (b_2, 30)	507.5	453.8
505	504 (b_2, 16)	465	441	469.1 (a_1, 9)	453.9	451.7

[a] Mode symmetry in C_{2v} point group: infrared intensity in km mol^{-1}. Normal isotopic frequencies. [b] Observed frequencies (argon matrix) listed for comparison. [c] $Th(^{13}C_2H_2)$ frequencies. [d] $Th(C_2D_2)$ frequencies.

Table 4. Frequencies [cm^{-1}] computed for the low lying $^1A'$ and $^3A''$ states of HThCCH and $^1A_1$ state of $ThCCH_2$ using DFT.

HThCCH $^1A'$			HThCCH $^3A''$	$ThCCH_2$ $^1A_1$
PW91	B3LYP	OBS	B3LYP	B3LYP
3364	3434 (51)[a]		3435 (58)[a]	3097 (b_2, 14)[a]
1932	2020 (33)		2005 (9)	3042 (a_1, 86)
1502	1515 (358)	1436[b]	1481 (468)	1652 (a_1, 87)
706	739 (33)		717 (41)	1438 (a_1, 6)
644	699 (39)		693 (40)	1026 (b_2, 8)
449	438 (83)		387 (100)	998 (b_1, 21)
352	348 (0.7)		–	492 (a_1, 39)

[a] Infrared intensities [km mol^{-1}]. [b] Observed frequency (argon matrix) listed for comparison.

The $Th(C_2H_2)^+$ cation in the $^2A_1$ state was found to be 560 kJ mol^{-1} higher than $^1A_1$ $Th(C_2H_2)$ at the B3LYP level. The strongest absorptions, the b_2 and b_1 bending modes, are 3 and 49 cm^{-1} higher than $^3A_2$ state neutral values. The $Th(C_2H_2)_2$ dimer was converged in a $^1A_1$ state of C_{2v} symmetry with a 105.2° angle between the two Th–C_2H_2 ligand planes. As expected, frequencies (Supporting Information, Table S1) are changed slightly from $Th(C_2H_2)$ values. Structural parameters for the two equivalent C_2H_2 ligands are Th–C 2.330 Å; angle C-Th-C 33.7°; C–H 1.091 Å; angle C-C-H 126.5°. Interestingly the b_2 and a_1 modes calculated at 521 and 469 cm^{-1} for $Th(C_2H_2)$ ($^3A_2$) split into strong b_1 (523 cm^{-1}) and b_2 (468 cm^{-1}) and weak a_1 (515 cm^{-1}) and forbidden a_2 (495 cm^{-1}) modes for $Th(C_2H_2)_2$.

The abundance of CCH radical in the spectrum suggested our consideration of the ThCCH product. Three low-lying ThCCH states computed are summarized in Table 5.

Similar DFT calculations were performed for three U + C_2H_2 isomers. The $^5A_1$ state of $U(C_2H_2)$, which appears to be the global minimum, is sketched in Figure 6; it is lower than the $^3A_2$ state by 25, 44 and 34 kJ mol^{-1}, respectively, at the B3LYP, B3PW91 and PW91 levels. The four unpaired electrons in $^5A_1$ $U(C_2H_2)$ are distributed in orbitals of a_1, a_2, b_1 and b_2 symmetries (one electron in each). In a formal sense, the electronic structure of $^5A_1$ $U(C_2H_2)$ may be derived from $^3A_2$ $Th(C_2H_2)$ by the addition of two unpaired electrons, to orbitals of b_1 and b_2 symmetries. Careful inspection of the MO of the two systems shows that the relationship is more than merely formal; the highest-lying doubly-occupied orbitals of $^5A_1$ $U(C_2H_2)$ are extremely similar to those of $^3A_2$ $Th(C_2H_2)$, as is the singly-occupied a_1 orbital. The a_2, b_1 and b_2 singly-occupied orbitals are essentially pure f-type atomic orbitals, very strongly localized on U, giving a spin density on U of 4.06 electrons. Given these close similarities in structure of the orbitals that correspond to M-acetylene interactions (M = Th or U), it is not surprising to find that the net charge on U in $^5A_1$ $U(C_2H_2)$ of +0.51 e (Mulliken) (or +1.36 e, NBO) is similar to that on Th in $^3A_2$ $Th(C_2H_2)$. The triplet-state calculations for $U(C_2H_2)$ suffered from severe spin-contamination, with values of $<S^2>$ being close to 2.9 for the apparently lowest-energy $^3A_2$ state (but for the quintet states, and for triplet $Th(C_2H_2)$, spin contamination was always

Table 5. Frequencies [cm^{-1}] calculated for the low lying $^2\Delta$, $^2\pi$, and $^4\Phi$ states of ThCCH using the B3LYP DFT.[a]

$^2\Delta$	OBS	$^2\Pi$	$^4\Phi$
3436 (σ, 61)[b]		3436 (σ, 74)[b]	3437 (σ, 100)[b]
2048 (σ, 143)	1938[c]	1983 (σ, 0.1)	1958 (σ, 31)
735 (π, 102)		760 (π, 75)	738 (π, 83)
731		647	605

[a] Bond lengths: $^2\Delta$ state 2.363, 1.221, 1.066 Å. $^2\Pi$ state 2.346, 1.225, 1.066 Å. $^4\Phi$ state 2.364, 1.227, 1.065 Å. [b] Mode symmetry in $C_{\infty v}$ point group: infrared intensity in km mol^{-1}. Normal isotopic frequencies. [c] Observed frequencies (argon matrix) listed for comparison.

negligible). We therefore do not report calculated vibrational data for these triplet states.

As there are many ways in which three electrons may be placed in the seven f-type orbitals, and as these orbitals are so spatially concentrated on the metal as to have little interaction with the acetylene ligand (see Discussion section), there are several quintet electronic states that are almost degenerate. In particular, a $^5A_2$ state, with unpaired electrons in a_1, a_1, b_1 and b_2 orbitals, is only 2 kJ mol^{-1} higher in energy than the $^5A_1$ state described above. In these circumstances, we obviously do not claim that our methods can identify the ground state with certainty, even in the spin-free approximation, but as the geometries of the two states are *extremely* similar, as are their calculated vibrational frequencies (differences typically of only 2–3 cm^{-1}), we feel that these uncertainties do not limit our use of the calculated vibrational frequencies to help assignment of the observed data. Table 6 summarizes frequency calculations for the $^5A_1$ state adduct. The quintet HUCCH insertion product is only 4 kJ mol^{-1} higher at the B3LYP level of theory, and the quintet $UCCH_2$ vinylidene is 26 kJ mol^{-1} higher. The most important vibrational bands for these two species are considered in the Discussion section.

Table 6. Frequencies [cm^{-1}] computed for the $^5A_1$ state of $U(C_2H_2)$ using DFT.

	PW91	
$U(C_2H_2)$	$U(^{13}C_2H_2)$	$U(C_2D_2)$
3038.7 (a_1, 39)	3027.9	2259.5
3009.2 (b_2, 25)	3000.2	2211.3
1351.4 (a_1, 10)	1301.4	1312.3
1079.9 (b_2, 43)	1063.4	905.2
946.1 (a_2, 0)	937.2	745.8
791.9 (a_1, 0.3)	790.9	567.9
611.1 (b_1, 41)	607.6	463.8
505.7 (b_2, 32)	492.0	441.7
446.8 (a_1, 21)	431.9	433.4
	B3LYP	
$U(C_2H_2)$	$U(^{13}C_2H_2)$	$U(C_2D_2)$
3093.4 (a_1, 53)	3082.8	2300.3
3062.8 (b_2, 31)	3054.3	2250.7
1406.9 (a_1, 5)	1354.5	1368.8
1133.4 (b_2, 40)	1116.6	944.6
996.6 (a_2, 0)	987.1	785.2
846.1 (a_1, 0.4)	844.9	607.6
621.9 (b_1, 45)	618.3	470.0
500.9 (b_2, 35)	487.0	439.7
485.0 (a_1, 50)	468.9	468.8

Discussion

The new Th and U product absorptions will be assigned on the basis of isotopic shifts and DFT frequency calculations. When comparing observed vibrational wavenumbers with the values calculated here, it is important to remember that the effects of vibrational anharmonicity, which are completely neglected in our calculations, are not negligible. In acetylene, the C–H stretching frequencies are lowered by 120–130 cm^{-1} (3.6%) by anharmonicity, while the triple-bond stretching frequency is lowered by nearly 40 cm^{-1} (1.8%).[53]

Th–η^2-(C_2H_2): The group A bands are assigned to $Th(C_2H_2)$, the thorium cyclopropene. The 2988.2 and 2946.2 cm^{-1} absorptions are due to the a_1 and b_2 C–H stretching modes. First, these bands are red-shifted 386 and 341 cm^{-1} from the σ_g and σ_u C–H stretching modes of C_2H_2.[15,16] The $^{12}C_2H_2/^{13}C_2H_2$ product frequency ratios, 1.00375 and 1.00271, respectively, are different for the a_1 and b_2 modes, as predicted by B3LYP calculations for the $^3A_2$ (1.00363 and 1.00298) and $^1A_1$ (1.00375 and 1.00294) states.

The important 1373.0 cm^{-1} band is assigned to the C=C stretching mode: this band is red-shifted 601 cm^{-1} from the C≡C stretching mode of acetylene. Unfortunately the $^{13}C=^{13}C$ stretching counterpart is calculated to appear at 1322 cm^{-1}, which is covered by the strong $\pi_g + \pi_u$ absorption of $^{13}C_2H_2$ at 1324 cm^{-1}; however, the C_2D_2 counterpart is observed at 1334.2 cm^{-1}. The C_2H_2/C_2D_2 frequency ratio 1373.0/1334.2 = 1.0292 is very nearly the frequency ratio 1.0298 predicted for the $^3A_2$ state but much below the 1.0349 ratio computed for the $^1A_1$ state.

The degenerate π_g and π_u bending vibrations of C_2H_2 at 612 and 729 cm^{-1} in the gas phase are computed to blue-shift substantially in $Th(C_2H_2)$, but only b_2 and b_1 modes have observable intensity, the b_2 mode predicted at 1126.1 cm^{-1} and the b_1 mode at 642.3 cm^{-1} ($^3A_2$ state, B3LYP). The sharp 1110.6 cm^{-1} absorption with 1.01471 and 1.1942 12/13 and H/D isotopic frequency ratios is assigned to the b_2 mode with computed 1.01579 and 1.1898 isotopic ratios, respectively (values for the $^1A_1$ state are almost the same). The 630.2 cm^{-1} band with 1.00784 and 1.3318 12/13 and H/D ratios is due to the b_1 mode with computed 1.00548 and 1.3232 isotopic frequency ratios, respectively. Although the b_2 and b_1 vibrations are both "C–H deformation modes," these normal coordinates involve very different C and H participations. Such is also the case for the π_g and π_u modes of C_2H_2.

Two important new vibrations in the $Th(C_2H_2)$ molecule are b_2 and a_1 Th–C stretching vibrations observed at 535.1 and 464.5 cm^{-1}. These are predicted at 521.7 and 469.4 cm^{-1} ($^3A_2$) and at 510.2 and 531.8 cm^{-1} ($^1A_1$), respectively, with 12/13 isotopic frequency ratios of 1.0280 and 1.0335, respectively (computed $^3A_2$ values given). The experimental 535.1 and 464.5 cm^{-1} bands exhibit different 1.0275 and 1.0331 ratios for 12/13, which are near the calculated b_2 and a_1 Th–C stretching modes in $Th(C_2H_2)$ in the order predicted for the triplet state and not the singlet state. Hence, we conclude that the triplet state for $Th(C_2H_2)$ is trapped in the argon matrix.

The $^1A_1$ and $^3A_2$ states for $Th(C_2H_2)$ are computed to be close in energy at the DFT level without spin-orbit coupling (less than 1 kJ mol^{-1} for PW91 and B3PW91, 22 kJ mol^{-1} for B3LYP, always in favor of the singlet). More sophisticated

single-reference methods also predict a singlet ground state: the singlet is lower than the triplet by 33 or 42 kJ mol^{-1} at the CCSD or CCSD(T) level of theory (CCSD-optimized geometries used, but these turn out to be very similar to those obtained at the B3LYP level, with no parameter differing by more than 0.6%. Since the T1 diagnostic is 0.025 for the singlet, the CCSD(T) method should be relatively reliable.[54]).

Multi-reference calculations were then undertaken, to provide more reliable predictions for the relative energies of the singlet and triplet states. A series of CASSCF calculations (8 electrons in nine orbitals) showed that the $^3A_2$ state is indeed clearly the lowest of the possible triplet states. The active space was then progressively increased to 14 electrons in 18 orbitals, and the singlet-triplet energy separation determined: note that 14 electrons corresponds to the full valence space of Th(C_2H_2). The singlet is found to be lower than the triplet by 48 $\pm$ 1 kJ mol^{-1}, for active spaces varying between (8,10) and (14,18). The energy separation is lowered slightly (by about 5–6 kJ mol^{-1}) by MR-CISD calculations, and our best estimate of the energy separation before considering spin-orbit coupling is 41 kJ mol^{-1}. The differential effects of spin-orbit coupling turn out to be remarkably small: the singlet manifold is preferentially stabilized by some 0.2 kJ mol^{-1}, a quantity smaller than the dispersion in our results as a function of the active space.

Since our MR-CISD and CCSD(T) values for the relative energies of the singlet and triplet states are so similar, at 41 or 42 kJ mol^{-1}, we feel confident that the ground state for Th(C_2H_2) in the gas phase is $^1A_1$, particularly since the effects of spin-orbit coupling are so small. However, the vibrational frequencies provide a clear basis of preference for the $^3A_2$ state for the molecule trapped in the argon matrix. Although many of the observed frequencies are predicted equally well for the two states (Table 3), the diagnostic low frequency b_2 and a_1 Th–(C_2H_2) stretching modes are computed much closer to the observed values (14 and 4 cm^{-1}) for the $^3A_2$ than for the $^1A_1$ state (25 and 68 cm^{-1}). Furthermore, more coupling is predicted for the two highest a_1 modes (sym C–H and C=C) for the $^1A_1$ state where the C=C mode is calculated higher (1478 cm^{-1}) than for the $^3A_2$ state where the C=C mode is computed lower (1381 cm^{-1}). It is important that the later is in much better agreement with the diagnostic 1373 cm^{-1} observed value. This is also manifest in the H/D ratio observed for the C=C stretching mode, 1373.0/1334.2 = 1.0291, and calculated for the $^3A_2$ state (1.0307) and in contrast to the $^1A_1$ state (1.0349). These vibrational frequency and isotopic shift comparisons support our preference for the $^3A_2$ state of Th(C_2H_2) trapped in solid argon.

This brings the CUO case back to mind, which has a singlet ground state recently calculated at the relativistic coupled-cluster level to be 58 kJ mol^{-1} lower than the triplet state.[34] However, the triplet state is observed in solid argon. The CUO(Ar)$_n$ complex in the triplet state is stabilized by more than the singlet complex such that the triplet argon complex is the ground state.[55] Thus, we believe the preferential stabilization for (Ar)$_n$(Th(C_2H_2)) in the triplet state is enough to reverse the calculated $^3A_2$ and $^1A_1$ order of states for Th(C_2H_2) in the solid argon matrix. This interaction with argon at the metal center is assisted by the higher charge computed for Th in the triplet than in the singlet state Th-(C_2H_2) and the higher dipole moment for the triplet state. Similar argon complexes have been observed and calculated recently for the UO_2^+ and Group 3 $M(OH)_2^+$ cations isolated in solid argon.[12,56] This is an interesting conclusion in its own right as it further underscores the principle that we are in fact dealing with argon complexes of guest molecules in the argon matrix environment, particularly guest molecules involving electropositive metal atoms.

The above vibrational frequencies for Th(C_2H_2), the substantially red-shifted C–H and C=C stretching modes and markedly blue-shifted C–H deformation modes relative to C_2H_2, and the high Th–C stretching frequencies all argue for a strong Th–C_2H_2 interaction. This is in accord with the substantial 284 kJ mol^{-1} binding energy estimated from B3LYP calculation without spin-orbit coupling, and the significant increase in the computed C–C distance compared with free acetylene. Furthermore, Reaction (1) is spontaneous based on the marked increase in absorption intensities on annealing solid argon into the 23–34 K range.

$$\mathrm{Th}\ (^3\mathrm{F}) + \mathrm{C_2H_2} \rightarrow \mathrm{Th(C_2H_2)}\ ^3\mathrm{A_2} \quad (1)$$

Th–η^2-(C_2H_2)$_2$: The group B bands fall in the same regions as the A bands and they behave similar to the group A bands except group B bands increase less on lower and more on higher temperature annealing than group A bands including the highest temperature annealing cycle where B bands slightly increase at the expense of A bands. In fact some of the B bands are very close to their A counterparts (609.7 vs 630.2 cm^{-1}, 535.9 vs 535.1 cm^{-1}, 488.7 vs 464.5 cm^{-1}). The C_2H_2 monomer absorptions decrease and $(C_2H_2)_x$ cluster bands increase on these annealing cycles. Thus, assignment of the B absorptions to Th(C_2H_2)$_2$ follows. Here we have two C_2H_2 molecules coordinated to Th as similarly found for Pd.[19] The C–H stretching modes at 2988 and 2962 cm^{-1} for species B are red-shifted from C_2H_2 slightly less than these modes for species A. Unfortunately, a C=C mode for Th(C_2H_2)$_2$ was not observed as this region is rich with strong Th–H stretching modes.

The C–H deformation region for Th(C_2H_2)$_2$ contains adsorptions at 1121.4 and 609.7 cm^{-1}, near the 1110.6 and 630.2 cm^{-1} bands for Th(C_2H_2). The Th–C stretching region contains two strong bands at 535.9 and 488.7 cm^{-1} with 12/13 ratios 1.0278 and 1.0330, almost the same as the 535.1 and 464.5 cm^{-1} bands for Th(C_2H_2). These are assigned to b_1 and b_2 out-of-phase combinations of stretching modes of the two Th-(C_2H_2) subunits. The in-phase combinations of these modes are not observed.

Computations find a C_{2v} structure for Th(C_2H_2)$_2$ of $^1A_1$ symmetry with computed frequencies (Supporting Information, Table S1) comparable to those for Th(C_2H_2) (Table 3).

Th–η²-(C_2H_2)$^+$: The group C bands at 1099.7 and 646.3 cm^{-1} increase and decrease on annealing cycles at lower temperature than group A bands. Hence these absorptions are due to a more reactive encounter and product species than Th(C_2H_2). Since the 1099.7 cm^{-1} band is only 10.9 cm^{-1} below the strongest Th(C_2H_2) absorption at 1110.6 cm^{-1}, the former could simply be due to a less stable matrix site. However, we expect Th^+ to be ablated and the Th(C_2H_2)$^+$ cation complex is a possibility. Our B3LYP calculations predict this mode 3 cm^{-1} higher than the corresponding mode for Th(C_2H_2). A possible associated band is observed at 641.3 cm^{-1}. We tentatively assign the 1099.7 cm^{-1} band to Th(C_2H_2)$^+$.

ThCCH: The 1937.6 cm^{-1} band increases on 23–33 K annealing then gives way to a stronger 1944.2 cm^{-1} absorption on 38–43 K annealing. The broader 1927 cm^{-1} electronic band is not associated with this absorption as the former shifts to 1868.2 cm^{-1} with $^{13}C_2H_2$ and to 1825.8 cm^{-1} with C_2D_2 while the latter electronic band remains unshifted. The 1937.6 cm^{-1} absorption shows 12/13 and H/D isotopic frequency ratios 1.0371 and 1.0612, respectively, which are in line with the 1.0338 and 1.0569 values for the CCH radical absorption at 1845.8 cm^{-1} and indicate a similar coupled C≡C and C–H stretching mode. The 1937.6 cm^{-1} band is assigned to ThCCH, thorium ethynyl, and the 1944.2 cm^{-1} band to the associated acetylene cluster ThCCH(C_2H_2)$_x$. Our B3LYP calculations find low-lying $^2\Delta$ and $^2\Pi$ states for ThCCH, and the former has a strong C≡C stretching mode computed at 2048 cm^{-1} but the latter has a very weak such mode computed at 1983 cm^{-1}. The energies of these two doublet states are very close: a B3LYP calculation favors the $^2\Pi$ state by 6 kJ mol^{-1}, but the $^2\Delta$ state is lower by just 3 kJ mol^{-1} at the CCSD level. Spin-orbit effects have been neglected in both these calculations, and it does not seem possible to assign the gas-phase ground state with confidence. The vibrational data argue in favor of a $^2\Delta$ state in the argon matrix. Our B3LYP calculation gave the (harmonic) C≡C mode for C_2H_2 at 2072 cm^{-1}, which is 98 cm^{-1} above the observed fundamental, so it is quite consistent to predict the C≡C mode for ThCCH 110 cm^{-1} too high.

Electronic absorptions: Preliminary TDDFT calculations neglecting the effects of spin-orbit coupling have been performed for the simplest thorium cluster, namely Th_2. We find a $^3\Sigma_u$ ground state (2.752 Å, 173 cm^{-1}) and a low-lying $^3\Delta_g$ state (2.663 Å, 192 cm^{-1}) approximately 1500 cm^{-1} higher. This is appropriate for d–d electronic transitions to be observed in the infrared region covered here. Although this is expected to be a weak electronic transition, we are dealing with the higher concentrations needed for IR spectra and such a weak electronic transition should be observable under these conditions. Similar observations have been made for titanium-containing species, and for the Ti_2 molecule itself in solid neon, though the ground state for Ti_2 is $^3\Delta_g$.[57,58]

U–η²-(C_2H_2): The six group A bands are assigned to uranium cyclopropene, U(C_2H_2). The 2944.4 and 2920.1 cm^{-1} absorptions are due to the a_1 and b_2 C–H stretching modes. The $^{12}C/^{13}C$ ratios, 1.00392 and 1.00292, are in accord with B3LYP predictions for the $^5A_1$ state modes (1.00357 and 1.00295), which is computed to be the ground state of the U(C_2H_2) complex at the DFT level of theory.

The diagnostic C=C stretching mode is masked by the strong 1330–1338 cm^{-1} C_2H_2 precursor absorption, but the $U^{13}C_2H_2$ and UC_2D_2 counterparts are observed at 1289.0 and 1303.8 cm^{-1}, respectively. Our DFT isotopic frequency calculations predict this mode at 1339 cm^{-1} based on shifts from the observed $U^{13}C_2H_2$ and UC_2D_2 fundamentals. After annealing to 43 K the C_2H_2 monomer absorption is removed in favor of (C_2H_2)$_x$ aggregate bands and a weak band is detected at 1337 cm^{-1}, which is probably due to the C=C fundamental of U(C_2H_2).

The observable components of the acetylene bending modes computed at 1135 and 634 cm^{-1} appeared for U(C_2H_2) at 1112.1 and 602.9 cm^{-1}. The sharp 1112.1 cm^{-1} band exhibits 1.0149 and 1.2128 values for the 12/13 and H/D isotopic frequency ratios, and it is assigned to the B_2 mode with computed 1.0152 and 1.2011 isotopic ratios, respectively, for the $^5A_1$ state. The 602.9 cm^{-1} band with the 12/13 ratio 1.00634 is due to the b_1 mode with 1.00635 computed ratio. Note that the a_2 and a_1 counterparts of these C–H bending modes are not observable (Table 6).

The important b_2 and a_1 U-C stretching vibrations are observed at 521.5 and 494.9 cm^{-1} with 1.0278 and 1.0369 12/13 and with 1.1392 and 1.0343 H/D ratios, which are in very good agreement with the computed 1.0289, 1.0344 and 1.1370, 1.0344 ratios, respectively. These "U–C" single-bond stretching frequencies are much lower than the 1047 cm^{-1} value observed for C≡U≡O.[5]

The uranium and acetylene reaction is spontaneous as the product absorptions increase on annealing 23–34 K in solid argon. The reaction is estimated to be 249 kJ mol^{-1} exothermic at the B3LYP level without spin-orbit coupling.

$$U + C_2H_2 \rightarrow U(C_2H_2)\ ^5A_1 \quad (2)$$

U–η²-(C_2H_2)$_2$: Two group B bands are near group A bands, but the B bands increase more on higher temperature annealing as C_2H_2 diffuses and aggregates these bands at 2970 and 1093.8 cm^{-1} are just above and below C–H stretching and bending modes for U(C_2H_2). Following the assignments to Th(C_2H_2)$_2$, the above B bands are most likely due to U(C_2H_2)$_2$.

U–η²-(C_2H_2)$^+$: The sharp 1106.1 cm^{-1} band appears on 23 K annealing, decreases at 28 K, and is gone after 34 K annealing when U(C_2H_2) is strongest. Hence the sharp 1106.1 cm^{-1} band is due to a more reactive species. We know that U^+ is evaporated in the laser ablation process as UO_2^+ has been observed in the matrix spectra,[4b] and accordingly the 1106.1 cm^{-1} band is tentatively assigned to U(C_2H_2)$^+$.

HUCCH: The strong 1392.6 and 1375.8 cm^{-1} bands observed on sample deposition increase on annealing and are accompanied by weaker 674.3 and 664.2 cm^{-1} absorptions. The former bands show no ^{13}C shift and a large H/D ratio (1.3997), hence they are due to U–H stretching modes as they fall in this region of the spectrum.[6] The former band increases at the expense of the latter on full arc photolysis: These two bands are believed to be matrix site absorptions of the same species. The 664.2 cm^{-1} band, on the other hand shows a 12/13 ratio 1.00927 and H/D ratio 1.261, which are appropriate for a CCH bending mode (the nearby CCH^+ band gives 1.0086 and 1.267 ratios, respectively). Isotopic counterparts could not be observed for the 674.3 cm^{-1} band. These absorptions are in good agreement with the strongest modes calculated for the quintet HUCCH insertion product at 1438 cm^{-1} (455 km mol^{-1}), 711 cm^{-1} (a″, 41 km mol^{-1}), 707 cm^{-1} (a′, 46 km mol^{-1}).

UCCH: The 1934.9 cm^{-1} band is strong on sample deposition, it increases on 23–28 K annealing while CCH radical decreases, and it decreases on 34–43 K annealing as isolated C_2H_2 is lost and blue satellites appear at 1942–1939 cm^{-1}. This feature exhibits 12/13 and H/D ratios 1.0362 and 1.0597, respectively, which are comparable to 1.0338 and 1.0569 values for the CCH radical at 1845.8 cm^{-1} and indicate a similar coupled C≡C and C–H stretching mode. On the other hand C_2H_2 itself exhibits 1.0335 and 1.0653 isotopic frequency ratios, and the latter shows the greater H–-D coupling for two bonded H(D) atoms. The 1934.9 cm^{-1} band is assigned to the UCCH uranium ethynyl species. Our B3LYP calculations find a $^4\Phi$ ground state with a strong C≡C stretching mode at 2026 cm^{-1}, which is in good agreement with our observation. Our calculated value is 91 cm^{-1} above the observed value whereas our calculated value for acetylene is 98 cm^{-1} above the experimental frequency.

The satellite bands which appear on annealing are attributed to the $UCCH(C_2H_2)_x$ cluster complex as acetylene diffuses and aggregates on annealing.

Metal ethynyl species have been observed in the C≡C stretching region for Pd (1988 cm^{-1}) and alkaline earth metals (Be, 2019 cm^{-1}; Mg, 1984 cm^{-1}), and Group 13 (B, 2039 cm^{-1}; Al, 1977 cm^{-1}).[16,48,59] Our 1938 and 1935 cm^{-1} observations for ThCCH and UCCH reveal a stronger interaction for carbon with the actinide metal atoms.

Comparisons of M–η^2-(C_2H_2) species: Vibrational data are now available for several M-(HCCH) systems which contain η^2-(C_2H_2), including M = Li, Ti, Ni, Pd and Pt,[15–20] as well as the cases of Th and U studied in this work (see Table 7). It is striking that the vibrational frequency of the C–C stretching mode is lower for U(HCCH) than for any other metal, implying that the interaction between uranium and acetylene is the strongest of all those studied to date. It is also remarkable that the vibrational and geometrical properties of Th(HCCH) and U-(HCCH) are so similar, despite the profound differences in ground-state electronic configurations of the two actinide atoms ($7s^2\ 6d^2$ for Th, $7s^2\ 6d^1\ 5f^3$ for U). When the overlap populations for $^5A_1$ U(HCCH) are analyzed in detail, we find that the predominant U–C interaction involves the 6d orbitals (of a total U–C overlap population of 0.241 at the B3LYP level, s orbitals on U contribute 0.029, d orbitals 0.226 and f orbitals only 0.047, the p orbitals giving an antibonding contribution of 0.061). The d–f balance is remarkably similar for $^3A_2$ Th(HCCH): 0.267 for d orbitals and 0.050 for f orbitals. It is not surprising that f-type orbitals on Th should be of little importance in bonding, but their small contribution in U(HCCH) might appear unexpected, given that they are lower in energy than 6d.

In fact, the dominant M–HCCH interaction concerns the π* C–C antibonding orbital, as has already been noted above. This orbital is clearly at higher energy than any occupied metal orbital, so the higher energy of the metal orbital, the better the energy-match criterion is satisfied, and the stronger the interaction expected. But the energy-match criterion is not the only important one: a strong interaction can occur only between orbitals of comparable sizes. The 5f orbitals on the actinides are *much* smaller than 6d, so when interactions over fairly long distances are concerned (note the Th–C and U–C distances in Figure 6 of nearly 2.3 Å), the participation of the 5f orbitals will be of only minor importance, as we have already noted when comparing the geometries of US_2 (bent) and UO_2 (linear).[4] It is informative to compare the energies and sizes of the valence orbitals for several metals. The data that follow are taken from the Tables prepared by Desclaux and are thus on a comparable basis.[60] We list orbital energies, in atomic units, followed by the expectation value of the orbital radii value, in Å: where necessary, we have averaged the values for the two components of different *J*: Th 6d, −0.217, 3.01; 7s, −0.209, 4.31: U 5f, −0.334, 1.44; 6d, −0.188, 3.22; 7s, −0.202, 4.34: Ti 3d, −0.397, 1.50: Pd 4d, −0.383, 1.54; Pt 5d, −0.421, 1.65.

Since the valence d orbitals for Pd and Pt are substantially lower in energy than those for Th or U, the analysis above implies that their interaction with acetylene will be weaker, as is indeed observed. The comparison of Ti with Th or U is more difficult: the orbital energy match with the π* C–C antibonding orbital appears less favorable for Ti than for the

Table 7. Comparison of vibrational frequencies [cm^{-1}] observed for several matrix-isolated M–η^2-C_2H_2 complexes in solid argon.

Mode	Li[a]	Ti[b]	Ni[c]	Pd[d]	Pt[e]	Th[f]	U[f]
C–H str.	2952.5	2968.1	(3112)			2946.6	2944.4
C–H str.	2909.7	2939.0	–			2920.2	2920.1
C–C str.	1655.0	1364.5	1647.4	1710	1654	1373.0	(1337)
C–H bend, in plane	714.0	1050.9	847.3	766	883	1110.6	1112.1
C–H bend, out plane	635.0	656.0	658.1	675	666	630.2	603
M–$(C)_2$ str.	479.7	573.0	548.6			464.5	512.3

[a] Ref. [11]. [b] Ref. [13]. [c] Ref. [14]. [d] Ref. [15]. [e] Ref. [16]. [f] this work.

actinides, but the sizes are quite different. It is also possible that the 4s orbital on Ti contributes appreciably to the interaction: its energy of −0.224 au is similar to that of the 6d orbitals on the actinides. Despite the nuclear charge being higher by two units, the 6d orbitals in U are slightly *higher* in energy than those in Th; presumably, in a one-electron picture they are strongly screened by the 5f electrons. This higher orbital energy is then consistent with a stronger interaction with acetylene, again following the analysis above.

Conclusion

Actinide metallacyclopropenes are formed in the spontaneous reaction of Th and U atoms with C_2H_2 on annealing in solid argon. The C–H and C=C stretching modes of C_2H_2 are red-shifted in Th(C_2H_2) and U(C_2H_2), but the C=C stretching mode is about 36 cm^{-1} lower, the C-H stretching mode 2.2 cm^{-1} lower, the C-C-H bending mode 1.5 cm^{-1} higher, and the a_1 M–C_2 stretching mode 30 cm^{-1} higher in the uranium compound, which indicates a slightly stronger interaction. Our DFT calculations yield vibrational frequencies that match the experimental data reasonably well. However, the calculations of binding energy, C≡C bond length and stretching frequency, in fact suggest a marginally stronger interaction in the Th species. We conclude that our neglect of spin-orbit coupling is probably responsible for these deficiencies. We analyze the C≡C stretching mode in a group of related metallacyclopropenes, including with the Li, In, Ti, Ni, Pd and Pt metals,[15–20] and draw attention to the importance of both orbital energies and orbital sizes. Finally, we find that the argon matrix interaction with Th(C_2H_2) is stronger with the $^3A_2$ than the $^1A_1$ state such that the order of states is reversed in the argon matrix for this $(Ar)_n$(Th(C_2H_2)) complex.

Acknowledgements

We gratefully acknowledge financial support from the National Science Foundation, exploratory experiments performed by R. D. Hunt, J. T. Lyon, and P. F. Souter, and the assistance of T. Leininger with the multireference calculations on Th(C_2H_2).

[1] M. Rashidi, R. J. Puddephatt, *J. Am. Chem. Soc.* **1986**, *108*, 7111.
[2] P. S. Cremer, S. D. Su, Y. R. Shen, G. A. Somorjai, *J. Phys. Chem. B* **1997**, *101*, 6474.
[3] R. Kose, W. A. Brown, D. A. King, *J. Am. Chem. Soc.* **1999**, *121*, 4845.
[4] a) R. D. Hunt, L. Andrews, *J. Chem. Phys.* **1993**, *98*, 3690; b) M. F. Zhou, L. Andrews, N. Ismail, C. Marsden, *J. Phys. Chem. A* **2000**, *104*, 5495; c) B. Liang, L. Andrews, N. Ismail, C. Marsden, *Inorg. Chem.* **2002**, *41*, 2811.
[5] G. P. Kushto, P. F. Souter, L. Andrews, M. Neurock, *J. Chem. Phys.* **1997**, *106*, 5894.
[6] P. F. Souter, G. P. Kushto, L. Andrews, M. Neurock, *J. Am. Chem. Soc.* **1997**, *119*, 1682.
[7] P. F. Souter, G. P. Kushto, L. Andrews, M. Neurock, *J. Phys. Chem. A* **1997**, *101*, 1287.
[8] M. F. Zhou, L. Andrews, J. Li, B. E. Bursten, *J. Am. Chem. Soc.* **1999**, *121*, 9712.
[9] B. Liang, L. Andrews, J. Li, B. E. Bursten, *J. Am. Chem. Soc.* **2002**, *124*, 9016.
[10] L. Andrews, B. Liang, J. Li, B. E. Bursten, *J. Am. Chem. Soc.* **2003**, *125*, 3126.
[11] B. Liang, L. Andrews, J. Li, B. E. Bursten, *Chem. Eur. J.* **2003**, *9*, 4781.
[12] X. Wang, L. Andrews, J. Li, B. E. Bursten, *Angew. Chem.* **2004**, *116*, 2608; *Angew. Chem. Int. Ed.* **2004**, *43*, 2554.
[13] B. Liang, L. Andrews, J. Li, B. E. Bursten, *Inorg. Chem.* **2004**, *43*, 882.
[14] L. Andrews, H.-G. Cho, *J. Phys. Chem. A* **2005**, *109*, 7696.
[15] L. Manceron, L. Andrews, *J. Am. Chem. Soc.* **1985**, *107*, 563 (Li + C_2H_2).
[16] T. R. Burkholder, L. Andrews, *Inorg. Chem.* **1993**, *32*, 2491 (Al, Ga, In + C_2H_2).
[17] L. Andrews, G. P. Kushto, unpublished results (Ti + C_2H_2).
[18] E. S. Kline, Z. H. Kafafi, R. H. Hauge, J. L. Margrave, *J. Am. Chem. Soc.* **1987**, *109*, 2402 (Ni + C_2H_2).
[19] X. Wang, L. Andrews, *J. Phys. Chem. A* **2003**, *107*, 337 (Pd + C_2H_2).
[20] X. Wang, L. Andrews, *J. Phys. Chem. A* **2004**, *108*, 4838 (Pt + C_2H_2).
[21] G. Herzberg, *Infrared and Raman Spectra of Polyatomic Molecules*, Van Nostrand, Princeton, **1945**.
[22] G. Strey, I. M. Mills, *J. Mol. Spectrosc.* **1976**, *59*, 103.
[23] G. P. Kushto, Ph.D. Thesis, University of Virginia, Charlottesville, Virginia, **1999**.
[24] L. Andrews, *Ann. Rev. Phys. Chem.* **1971**, *22*, 109, and references therein.
[25] N. Ismail, J.-L. Heully, T. Saue, J.-P. Daudey, D. J. Marsden, *Chem. Phys. Lett.* **1999**, *300*, 296.
[26] L. Gagliardi, B. O. Roos, P. A. Malmqvist, J. M. Dyke, *J. Phys. Chem. A* **2001**, *105*, 10602.
[27] S. Tsushima, T. Reich, *Chem. Phys. Lett.* **2001**, *347*, 127.
[28] M. Straka, K. G. Dyall, P. Pyykko, *Theor. Chem. Acc.* **2001**, *106*, 393.
[29] C. Clavaguera-Sarrio, S. Hoyau, N. Ismail, C. J. Marsden, *J. Phys. Chem. A* **2003**, *107*, 4515.
[30] C. Clavaguera-Sarrio, V. Vallet, D. Maynau, C. J. Marsden, *J. Chem. Phys.* **2004**, *121*, 5312.
[31] A. Kovacs, R. J. M. Konings, *J. Mol. Struct.* **2004**, *684*, 35.
[32] H. P. Hratchen, J. L. Sonnenberg, J. P. Hay, R. L. Martin, B. E. Bursten, H. B. Schlagel, *J. Phys. Chem. A* **2005**, *109*, 8579.
[33] J. L. Sonnenberg, J. P. Hay, R. L. Martin, B. E. Bursten, *Inorg. Chem.* **2005**, *44*, 2255.
[34] I. Infante, L. Visscher, *J. Chem. Phys.* **2004**, *121*, 5783.
[35] L. Gagliardi, P. Pyykko, B. O. Roos, *Phys. Chem. Chem. Phys.* **2005**, *7*, 2415.
[36] L. Gagliardi, B. O. Roos, *Nature* **2005**, *433*, 848.
[37] B. O. Roos, L. Gagliardi, *Inorg. Chem.* **2006**, *45*, 803.
[38] L. Andrews, *Chem. Soc. Rev.* **2004**, *33*, 123, and references therein.
[39] a) Gaussian 03, Revision B.04, M. J. Frisch, G. W. Trucks, H. B. Schlegel, G. E. Scuseria, M. A. Robb, J. R. Cheeseman, J. A. Jr. Montgomery, T. Vreven, K. N. Kudin, J. C. Burant, J. M. Millam, S. S. Iyengar, J. Tomasi, V. Barone, B. Mennucci, M. Cossi, G. Scalmani, N. Rega, G. A. Petersson, H. Nakatsuji, M. Hada, M. Ehara, K. Toyota, R. Fukuda, J. Hasegawa, M. Ishida, T. Nakajima, Y. Honda, O. Kitao, H. Nakai, M. Klene, X. Li, J. E. Knox, H. P. Hratchian, J. B. Cross, C. Adamo, J. Jaramillo, R. Gomperts, R. E. Stratmann, O. Yazyev, A. J. Austin, R. Cammi, C. Pomelli, J. W. Ochterski, P. Y. Ayala, K. Morokuma, G. A. Voth, P. Salvador, J. J. Dannenberg, V. G. Zakrzewski, S. Dapprich, A. D. Daniels, M. C. Strain, O. Farkas,. Malick, D. K; A. D. Rabuck, K. Raghavachari, J. B. Foresman, J. V. Ortiz, Q. Cui, A. G. Baboul, S. Clifford, J. Cioslowski, B. B. Stefanov, G. Liu, A. Liashenko, P. Piskorz, I. Komaromi, R. L. Martin, D. J. Fox,.T. Keith, M. A. Al-Laham, C. Y. Peng, A. Nanayakkara, M. Challacombe, P. M. W. Gill, B. Johnson, W. Chen, M. W. Wong, C. Gonzalez, J. A. Pople, Gaussian, Inc., Pittsburgh PA, **2003**, and references therein; b) P. J. Stevens, F. J. Devlin,

C. F. Chablowski, M. J. Frisch, *J. Phys. Chem.* **1994**, *98*, 11623; c) R. Krishnan, J. S. Binkley, R. Seeger, J. A. Pople, *J. Chem. Phys.* **1980**, *72*, 650; M. J. Frisch, J. A. Pople, J. S. Binkley, *J. Chem. Phys.* **1984**, *80*, 3265; d) D. Andrae, U. Haussermann, M. Daly, H. Stoll, H. Preuss, *Theor. Chim. Acta* **1990**, *88*, 123; e) T. Van Voorhis, G. E. Scuseria, *J. Chem. Phys.* **1998**, *109*, 400.

[40] T. H. Dunning, *J. Chem. Phys.* **1971**, *55*, 716.

[41] W. Kuchle, M. Dolg, H. Stoll, H. Preuss, *J. Chem. Phys.* **1994**, *100*, 7535.

[42] C. Lee, E. Yang, R. G. Parr, *Phys. Rev. B* **1988**, 37, 785; A. D. Becke, *J. Chem. Phys.* **1993**, *98*, 5648.

[43] J. P. Perdew, J. A. Chevary, S. H. Vosko, K. A. Jackson, M. R. Pederson, D. J. Singh, C. Fiolhais, *Phys. Rev. B* **1992**, *46*, 6671.

[44] G. D. Purvis, R. J. Bartlett, *J. Chem. Phys.* **1982**, *76*, 1910.

[45] MOLPRO, a package of ab initio programs designed by H.-J. Werner and P. J. Knowles, version 2002.6, R. D. Amos, A. Bernhardsson, A. Berning, P. Celani, D. L. Cooper, M. J. O. Deegan, A. J. Dobbyn, F. Eckert, C. Hampel, G. Hetzer, P. J. Knowles, T. Korona, R. Lindh, A. W. Lloyd, S. J. McNicholas, F. R. Manby, W. Meyer, M. E. Mura, A. Nicklass, P. Palmieri, R. Pitzer, G. Rauhut, M. Schütz, U. Schumann, H. Stoll, A. J. Stone, R. Tarroni, T. Thorsteinsson, H.-J. Werner.

[46] M. E. Jacox, *Chem. Phys.* **1975**, *7*, 424.

[47] L. Andrews, G. P. Kushto, M. Zhou, S. P. Willson, P. F. Souter, *J. Chem. Phys.* **1999**, *110*, 4457.

[48] C. A. Thompson, L. Andrews, *J. Am. Chem. Soc.* **1996**, *118*, 10242 (Be, Mg + C_2H_2).

[49] M. E. Jacox, *J. Phys. Chem. Ref. Data* **1994**, *23*, 32, and references therein.

[50] D. E. Milligan, M. E. Jacox, *J. Chem. Phys.* **1969**, *51*, 277.

[51] R. S. Mulliken, *J. Chem. Phys.* **1955**, *23*, 1833.

[52] J. E. Carpenter, F. Weinhold, *J. Mol. Struct.* **1988**, *169*, 41.

[53] J. M. L. Martin, T. J. Lee, P. R. Taylor, *J. Chem. Phys.* **1998**, *108*, 676.

[54] T. J. Lee, P. R. Taylor, *Int. J. Quantum Chem. Symp.* **1989**, *23*, 199.

[55] a) J. Li, B. E. Bursten, B. Liang, L. Andrews, *Science* **2002**, *295*, 2242; b) B. Liang, L. Andrews, J. Li, B. E. Bursten, *Chem. Eur. J.* **2003**, *9*, 4781; c) B. Liang, L. Andrews, J. Li, B. E. Bursten, *Inorg. Chem.* **2004**, *43*, 882.

[56] X. Wang, L. Andrews, *J. Phys. Chem. A* **2006**, *110*, 1850 (Group 3 $M(OH)_2^+$).

[57] H.-G. Cho, L. Andrews, *J. Phys. Chem. A* **2004**, *108*, 6294 (Ti + CH_3F).

[58] Hübner, H.-J. Himmel, L. Manceron, W. Klopper, *J. Chem. Phys.* **2004**, *121*, 7195.

[59] a) J. M. L. Martin, P. R. Taylor, P. Hassanzadeh, L. Andrews, *J. Am. Chem. Soc.* **1993**, *115*, 2510; b) L. Andrews, P. Hassanzadeh, J. M. L. Martin, P. R. Taylor, *J. Phys. Chem.* **1993**, *97*, 5839 (B + C_2H_2); c) G. V. Chertihin, L. Andrews, P. R. Taylor, *J. Am. Chem. Soc.* **1994**, *116*, 3513 (Al + C_2H_2).

[60] J. P. Desclaux, *At. Data Nucl. Data Tables* **1973**, *12*, (4).

Received: January 17, 2006
Revised: April 10, 2006
Published online: August 25, 2006

